

# Chiral symmetry restoration in strange hadronic matter

P. Wang, V. E. Lyubovitskij, Th. Gutsche, and Amand Faessler  
*Institut für Theoretische Physik, Universität Tübingen, Auf der Morgenstelle 14,  
D-72076 Tübingen, Germany*

## Abstract

The phase transition of chiral symmetry restoration in strange hadronic matter is studied in the chiral SU(3) quark mean field model. When the baryon density is larger than a critical density  $\rho_c$ , the minimal energy density of the system occurs at the point where the effective masses of nucleon,  $\Lambda$  or  $\Xi$  drop to zero. The physical quantities change discontinuously at this density and the system will be in the phase of chiral symmetry restoration. A rich phase structure of strange hadronic matter with different strangeness fraction  $f_s$  is obtained.

PACS number(s): 21.65.+f; 12.39.-x; 11.30.Rd

Keywords: chiral symmetry, quark mean field, strange matter, phase transition

## I. INTRODUCTION

It is generally believed that there are two phase transitions in hot and dense hadronic matter [1,2]. One is deconfinement which is related to the transition from hadronic to quark matter and the other is the chiral symmetry restoration. Lattice QCD simulations show that chiral symmetry restoration and deconfinement occur at the same critical temperature  $T_c$  [3]. The qualitative feature that at high temperature deconfinement and chiral symmetry restoration come together is not much of a mystery: in the deconfinement phase quarks are hypothetically free and their masses tend to zero. It is a longstanding puzzle however why deconfinement and chiral symmetry restoration occur quantitatively at the same temperature, though there are some explanations to connect these two phase transitions [4].

Some of the signals related to the appearance of the deconfined phase are the phenomenon of strangeness enhancement and the  $J/\Psi$  suppression [5,6]. A direct signature of the formation of the deconfined phase is the existence of strangelets. Many ultrarelativistic heavy-ion collision experiments at Brookhaven and CERN are proposed to search for (meta)stable lumps of such kind of strangelets. Up to now, there is no experiment which confirms the existence of strangelets. Ardouin et al. [7] presented a novel method which can be applied to characterize the possible existence of a strange quark matter distillation process in heavy-ion collisions. Asakawa et al. [8] pointed out that the size of the average fluctuations of net baryon number and electric charge in a finite volume of hadronic matter differs widely between the confined and deconfined phases which in turn can be exploited

as indicators for the formation of a quark-gluon plasma in relativistic heavy-ion collisions. The E864 collaboration found that there was no evidence for neutral strangelet production in 11.5 GeV/c per nucleon Au+Pb collisions [9]. The new measurement of NA50 revealed a steady significant decrease in the  $J/\Psi$  production rate up to the most central Pb-Pb collisions and it clearly rules out the presently available conventional (hadronic) models of  $J/\Psi$  suppression. This new observation leads to a natural explanation in the framework of the formation of a deconfined state of quarks and gluons [10].

In the context of the present work we investigate whether chiral symmetry restoration occurs only when quarks are deconfined, i.e., whether the phase transition of chiral symmetry restoration can appear in hadronic matter. In Ref. [11], it was pointed out that chiral symmetry breaking will strengthen in nuclear matter. Furthermore, the quark condensate will increase with baryon density for values higher than about  $0.7\rho_0$ , where  $\rho_0$  is the saturation density of nuclear matter. The quark condensate in the nuclear medium has also been evaluated in the framework of mean-field theory, the Nambu-Jona-Lasinio model, the relativistic Brueckner Hartree-Fock approach, and the bare vertex nuclear Schwinger-Dyson formalism [12]- [15]. The results of these models indicate that the quark condensate in nuclear matter is considerably reduced already for saturation density. The effect of chiral symmetry restoration can also be connected to the effective baryon mass [16]. Calculations from nuclear models show that the effective nucleon mass will decrease in nuclear matter.

Presently, lattice calculation cannot be applied to systems with finite baryon density, we therefore have to resort even more to phenomenological models to investigate hadronic matter. The symmetries of QCD can be used as a guideline to determine largely how the hadrons should interact with each other. Following this idea, models based on  $SU(2)_L \times SU(2)_R$  symmetry and scale invariance were proposed. These effective models have been widely used in the last years to investigate nuclear matter and finite nuclei both at zero and at finite temperature [17]- [23]. Papazoglou et al. extended the effective chiral models to  $SU(3)_L \times SU(3)_R$  including the full baryon octet [24,25]. Although these chiral models indicate that the effective nucleon mass decreases with density, there is no phase transition with respect to chiral symmetry restoration. As an extension we proposed the chiral  $SU(3)$  quark mean field model and investigated hadronic and quark matter [26]- [28]. The chiral symmetry restoration of nuclear matter was also studied in this model and a phase transition was found [29]. At some critical baryon density, the effective nucleon mass and the quark condensate decrease discontinuously. In the present work we will extend the investigation to study chiral symmetry restoration of strange hadronic matter which includes  $\Lambda$ ,  $\Sigma$  and  $\Xi$  hyperons.

The paper is organized as follows. The basic features of the model are introduced in Sec. II. In Sec. III, we use this model to investigate chiral symmetry restoration of strange hadronic matter. In Sec. IV we present the numerical results. In Sec. V we summarize our conclusions.

## II. THE MODEL

Our considerations are based on the chiral  $SU(3)$  quark mean field model (for details see Refs. [26,27]), which contains quarks and mesons as basic degrees of freedom. Quarks are confined into baryons by an effective potential. The quark meson interaction and meson

self-interaction are based on the SU(3) chiral symmetry. Through the mechanism of spontaneous chiral symmetry breaking, the resulting constituent quarks and mesons (except for the pseudoscalar ones) obtain masses. The introduction of an explicit symmetry breaking term in the meson self-interaction generates the masses of the pseudoscalar mesons which satisfy the PCAC relation. The explicit symmetry breaking term of the quark meson interaction leads in turn to reasonable hyperon potentials in hadronic matter. For completeness, we introduce the main concepts of the model in this section.

In the chiral limit, the quark field  $q$  can be split into left and right-handed parts  $q_L$  and  $q_R$ :  $q = q_L + q_R$ . Under  $SU(3)_L \times SU(3)_R$  they transform as

$$q_L \rightarrow q'_L = L q_L, \quad q_R \rightarrow q'_R = R q_R. \quad (1)$$

The spin-0 mesons are written in the compact form

$$M(M^+) = \Sigma \pm i\Pi = \frac{1}{\sqrt{2}} \sum_{a=0}^8 (s^a \pm ip^a) \lambda^a, \quad (2)$$

where  $s^a$  and  $p^a$  are the nonets of scalar and pseudoscalar mesons, respectively,  $\lambda^a$  ( $a = 1, \dots, 8$ ) are the Gell-Mann matrices, and  $\lambda^0 = \sqrt{\frac{2}{3}} I$ . The alternatives, plus and minus signs correspond to  $M$  and  $M^+$ . Under chiral SU(3) transformations,  $M$  and  $M^+$  transform as  $M \rightarrow M' = LMR^+$  and  $M^+ \rightarrow M^{+'} = RM^+L^+$ . As for the spin-0 mesons, the spin-1 mesons are set up in a similar way as

$$l_\mu(r_\mu) = \frac{1}{2} (V_\mu \pm A_\mu) = \frac{1}{2\sqrt{2}} \sum_{a=0}^8 (v_\mu^a \pm a_\mu^a) \lambda^a \quad (3)$$

with the transformation properties:  $l_\mu \rightarrow l'_\mu = Ll_\mu L^+$ ,  $r_\mu \rightarrow r'_\mu = Rr_\mu R^+$ . The matrices  $\Sigma$ ,  $\Pi$ ,  $V_\mu$  and  $A_\mu$  can be written in a form where the physical states are explicit. For the scalar and vector nonets, we have the expressions

$$\Sigma = \frac{1}{\sqrt{2}} \sum_{a=0}^8 s^a \lambda^a = \begin{pmatrix} \frac{1}{\sqrt{2}} (\sigma + a_0^0) & a_0^+ & K^{*+} \\ a_0^- & \frac{1}{\sqrt{2}} (\sigma - a_0^0) & K^{*0} \\ K^{*-} & \bar{K}^{*0} & \zeta \end{pmatrix}, \quad (4)$$

$$V_\mu = \frac{1}{\sqrt{2}} \sum_{a=0}^8 v_\mu^a \lambda^a = \begin{pmatrix} \frac{1}{\sqrt{2}} (\omega_\mu + \rho_\mu^0) & \rho_\mu^+ & K_\mu^{*+} \\ \rho_\mu^- & \frac{1}{\sqrt{2}} (\omega_\mu - \rho_\mu^0) & K_\mu^{*0} \\ K_\mu^{*-} & \bar{K}_\mu^{*0} & \phi_\mu \end{pmatrix}. \quad (5)$$

Pseudoscalar and pseudovector nonet mesons can be written in a similar fashion.

The total effective Lagrangian is set up as

$$\mathcal{L}_{\text{eff}} = \mathcal{L}_{q0} + \mathcal{L}_{qM} + \mathcal{L}_{\Sigma\Sigma} + \mathcal{L}_{VV} + \mathcal{L}_{\chi SB} + \mathcal{L}_{\Delta m_s} + \mathcal{L}_h + \mathcal{L}_c, \quad (6)$$

where  $\mathcal{L}_{q0} = \bar{q} i\gamma^\mu \partial_\mu q$  is the free part for massless quarks. The quark-meson interaction  $\mathcal{L}_{qM}$  can be written in a chiral SU(3) invariant way as

$$\begin{aligned}
\mathcal{L}_{qM} &= g_s \left( \bar{\Psi}_L M \Psi_R + \bar{\Psi}_R M^+ \Psi_L \right) - g_v \left( \bar{\Psi}_L \gamma^\mu l_\mu \Psi_L + \bar{\Psi}_R \gamma^\mu r_\mu \Psi_R \right) \\
&= \frac{g_s}{\sqrt{2}} \bar{\Psi} \left( \sum_{a=0}^8 s_a \lambda_a + i \gamma^5 \sum_{a=0}^8 p_a \lambda_a \right) \Psi - \frac{g_v}{2\sqrt{2}} \bar{\Psi} \left( \gamma^\mu \sum_{a=0}^8 v_\mu^a \lambda_a - \gamma^\mu \gamma^5 \sum_{a=0}^8 a_\mu^a \lambda_a \right) \Psi. \quad (7)
\end{aligned}$$

In the mean field approximation, the chiral-invariant scalar meson  $\mathcal{L}_{\Sigma\Sigma}$  and vector meson  $\mathcal{L}_{VV}$  self-interaction terms are written as [26,27]

$$\begin{aligned}
\mathcal{L}_{\Sigma\Sigma} &= -\frac{1}{2} k_0 \chi^2 (\sigma^2 + \zeta^2) + k_1 (\sigma^2 + \zeta^2)^2 + k_2 \left( \frac{\sigma^4}{2} + \zeta^4 \right) + k_3 \chi \sigma^2 \zeta \\
&\quad - k_4 \chi^4 - \frac{1}{4} \chi^4 \ln \frac{\chi^4}{\chi_0^4} + \frac{\delta}{3} \chi^4 \ln \frac{\sigma^2 \zeta}{\sigma_0^2 \zeta_0}, \quad (8)
\end{aligned}$$

$$\mathcal{L}_{VV} = \frac{1}{2} \frac{\chi^2}{\chi_0^2} \left( m_\omega^2 \omega^2 + m_\rho^2 \rho^2 + m_\phi^2 \phi^2 \right) + g_4 \left( \omega^4 + 6\omega^2 \rho^2 + \rho^4 + 2\phi^4 \right), \quad (9)$$

where  $\delta = 6/33$ ;  $\sigma_0$ ,  $\zeta_0$  and  $\chi_0$  are the vacuum expectation values of the corresponding mean fields  $\sigma$ ,  $\zeta$  and  $\chi$ . The Lagrangian  $\mathcal{L}_{\chi SB}$  generates the nonvanishing masses of pseudoscalar mesons

$$\mathcal{L}_{\chi SB} = \frac{\chi^2}{\chi_0^2} \left[ m_\pi^2 F_\pi \sigma + \left( \sqrt{2} m_K^2 F_K - \frac{m_\pi^2}{\sqrt{2}} F_\pi \right) \zeta \right], \quad (10)$$

leading to a nonvanishing divergence of the axial currents which in turn satisfy the PCAC relations for  $\pi$  and  $K$  mesons. Pseudoscalar, scalar mesons and also the dilaton field  $\chi$  obtain mass terms by spontaneous breaking of chiral symmetry in the Lagrangian (8). The masses of  $u$ ,  $d$  and  $s$  quarks are generated by the vacuum expectation values of the two scalar mesons  $\sigma$  and  $\zeta$ . To obtain the correct constituent mass of the strange quark, an additional mass term has to be added:

$$\mathcal{L}_{\Delta m_s} = -\Delta m_s \bar{q} S q \quad (11)$$

where  $S = \frac{1}{3} (I - \lambda_8 \sqrt{3}) = \text{diag}(0, 0, 1)$  is the strangeness quark matrix. Based on above mechanisms, the quark constituent masses are finally given by

$$m_u = m_d = -\frac{g_s}{\sqrt{2}} \sigma_0 \quad \text{and} \quad m_s = -g_s \zeta_0 + \Delta m_s. \quad (12)$$

In order to obtain reasonable hyperon potentials in hadronic matter we include an additional coupling between strange quarks and the scalar mesons  $\sigma$  and  $\zeta$  [26]. This term is expressed as

$$\mathcal{L}_h = (h_1 \sigma + h_2 \zeta) \bar{s} s. \quad (13)$$

In the quark mean field model, quarks are confined in baryons by the Lagrangian  $\mathcal{L}_c = -\bar{\Psi} \chi_c \Psi$ . The Dirac equation for a quark field  $\Psi_{ij}$  under the additional influence of the meson mean fields is given by

$$\left[ -i \vec{\alpha} \cdot \vec{\nabla} + \chi_c + \beta m_i^* \right] \Psi_{ij} = e_i^* \Psi_{ij}, \quad (14)$$

where the subscripts  $i$  and  $j$  denote the quark  $i$  ( $i = u, d, s$ ) in a baryon of type  $j$  ( $j = N, \Lambda, \Sigma, \Xi$ ). The constants  $m_i^*$  and  $e_i^*$  are defined as

$$m_i^* = -g_\sigma^i \sigma - g_\zeta^i \zeta + m_{i0} \quad (15)$$

and

$$e_i^* = e_i - g_\omega^i \omega - g_\phi^i \phi, \quad (16)$$

where  $e_i$  is the energy of the quark under the influence of the meson mean fields. The confining potential is chosen to be  $\chi_c^C$  as a combination of scalar and scalar-vector potentials as in Ref. [27,29]:

$$\chi_c^C = \frac{1}{2}(\chi_c^A + \chi_c^B) \quad (17)$$

with

$$\chi_c^A = \frac{1}{4}kr^2(1 + \gamma^0) \quad (18)$$

and

$$\chi_c^B = \frac{1}{4}kr^2. \quad (19)$$

As deduced from the Dirac equation (14) the effective mass of the baryon  $j$  is

$$M_j^{*2} = \sqrt{E_j^{*2} - \langle p_{j\,cm}^2 \rangle}, \quad (20)$$

where the energy  $E_j^* = \sum_i n_{ij} e_i^* + E_{j\,spin}$  and  $\langle p_{j\,cm}^2 \rangle$  is the spurious center of mass motion. In the expression for the baryon energy  $n_{ij}$  is the number of quarks  $i$  in baryon  $j$  and  $E_{j\,spin}$  is determined from a fit to the baryon masses:  $M_N = 939$  MeV,  $M_\Lambda = 1116$  MeV,  $M_\Sigma = 1196$  MeV and  $M_\Xi = 1331$  MeV.

### III. STRANGE HADRONIC MATTER

Based on the previously defined quark mean field model the Lagrangian density for strange hadronic systems is written as

$$\begin{aligned} \mathcal{L} = & \bar{\psi}_B (i\gamma^\mu \partial_\mu - M_B^*) \psi_B + \frac{1}{2} \partial_\mu \sigma \partial^\mu \sigma + \frac{1}{2} \partial_\mu \zeta \partial^\mu \zeta + \frac{1}{2} \partial_\mu \chi \partial^\mu \chi - \frac{1}{4} F_{\mu\nu} F^{\mu\nu} - \frac{1}{4} S_{\mu\nu} S^{\mu\nu} \\ & - g_\omega^B \omega_\mu \bar{\psi}_B \gamma^\mu \psi_B - g_\phi^B \phi_\mu \bar{\psi}_B \gamma^\mu \psi_B + \mathcal{L}_M, \end{aligned} \quad (21)$$

where

$$F_{\mu\nu} = \partial_\mu \omega_\nu - \partial_\nu \omega_\mu \quad \text{and} \quad S_{\mu\nu} = \partial_\mu \phi_\nu - \partial_\nu \phi_\mu. \quad (22)$$

The term  $\mathcal{L}_M$  represents the interaction between mesons which includes the scalar meson self-interaction  $\mathcal{L}_{\Sigma\Sigma}$ , the vector meson self-interaction  $\mathcal{L}_{VV}$  and the explicit chiral symmetry

breaking term  $\mathcal{L}_{\chi SB}$ , all defined previously. The Lagrangian includes the scalar mesons  $\sigma$ ,  $\zeta$  and  $\chi$ , and the vector mesons  $\omega$  and  $\phi$ . The interactions between quarks and scalar mesons result in the effective baryon masses  $M_B^*$ , where subscript  $B$  labels the baryon  $B = N, \Lambda, \Sigma$  or  $\Xi$ . The interactions between quarks and vector mesons generate the baryon-vector meson interaction terms of equation (21). The corresponding vector coupling constants  $g_\omega^B$  and  $g_\phi^B$  are baryon dependent and satisfy the SU(3) relationship. As originally set up by the interaction of quarks and vector mesons, on the hadron level we can get the following relations of the vector coupling constants:

$$g_\omega^\Lambda = g_\omega^\Sigma = 2g_\omega^\Xi = \frac{2}{3}g_\omega^N \quad \text{and} \quad g_\phi^\Lambda = g_\phi^\Sigma = \frac{1}{2}g_\phi^\Xi = \frac{\sqrt{2}}{3}g_\phi^N. \quad (23)$$

At finite temperature and density, the thermodynamical potential is defined as

$$\Omega = - \sum_{j=N,\Lambda,\Sigma,\Xi} \frac{g_j k_B T}{(2\pi)^3} \int_0^\infty d^3k \left\{ \ln \left( 1 + e^{-(E_j^*(k) - \nu_j)/k_B T} \right) + \ln \left( 1 + e^{-(E_j^*(k) + \nu_j)/k_B T} \right) \right\} - \mathcal{L}_M, \quad (24)$$

where  $E_j^*(k) = \sqrt{M_j^{*2} + k^2}$  and  $g_j$  is the degeneracy of baryon  $j$  ( $g_{N,\Xi} = 2$ ,  $g_\Lambda = 1$  and  $g_\Sigma = 3$ ). The quantity  $\nu_j$  is related to the usual chemical potential  $\mu_j$  by

$$\nu_j = \mu_j - g_\omega^j \omega - g_\phi^j \phi. \quad (25)$$

At zero temperature, the thermodynamical potential of symmetric hadronic matter can be expressed as

$$\Omega = \sum_{j=N,\Lambda,\Sigma,\Xi} \frac{g_j}{12\pi^2} \left\{ \nu_j \left[ \nu_j^2 - M_j^{*2} \right]^{1/2} \left[ 2\nu_j^2 - 5M_j^{*2} \right] + 3M_j^{*4} \ln \left[ \frac{\nu_j + (\nu_j^2 - M_j^{*2})^{1/2}}{M_j^*} \right] \right\} - \mathcal{L}_M. \quad (26)$$

The energy per volume and the pressure of the system can be derived as  $\varepsilon = \Omega + \nu_j \rho_j$  and  $p = -\Omega$ , where  $\rho_j$  is the baryon density.

The mean field equation for meson  $\phi_i$  is obtained by the formula  $\frac{\partial \Omega}{\partial \phi_i} = 0$ . For example, the equations for  $\sigma$ ,  $\zeta$  are deduced as:

$$k_0 \chi^2 \sigma - 4k_1 (\sigma^2 + \zeta^2) \sigma - 2k_2 \sigma^3 - 2k_3 \chi \sigma \zeta - \frac{2\delta}{3\sigma} \chi^4 + \frac{\chi^2}{\chi_0^2} m_\pi^2 F_\pi - \left( \frac{\chi}{\chi_0} \right)^2 m_\omega \omega^2 \frac{\partial m_\omega}{\partial \sigma} + \sum_{j=N,\Lambda,\Sigma,\Xi} \frac{\partial M_j^*}{\partial \sigma} \langle \bar{\psi}_j \psi_j \rangle = 0, \quad (27)$$

$$k_0 \chi^2 \zeta - 4k_1 (\sigma^2 + \zeta^2) \zeta - 4k_2 \zeta^3 - k_3 \chi \sigma^2 - \frac{\delta}{3\zeta} \chi^4 + \frac{\chi^2}{\chi_0^2} \left( \sqrt{2} m_k^2 F_k - \frac{1}{\sqrt{2}} m_\pi^2 F_\pi \right) - \left( \frac{\chi}{\chi_0} \right)^2 m_\phi \phi^2 \frac{\partial m_\phi}{\partial \zeta} + \sum_{j=\Lambda,\Sigma,\Xi} \frac{\partial M_j^*}{\partial \zeta} \langle \bar{\psi}_j \psi_j \rangle = 0, \quad (28)$$

where

$$\langle \bar{\psi}_j \psi_j \rangle = \frac{g_j}{\pi^2} \int_0^{k_{jF}} dk \frac{k^2 M_j^*}{\sqrt{M_j^{*2} + k^2}}, \quad (29)$$

with  $k_{jF} = \sqrt{\nu_j^2 - M_j^{*2}}$ . At zero baryon density, the vacuum expectation values of  $\sigma$  and  $\zeta$  are given as

$$\sigma_0 = -F_\pi, \quad \zeta_0 = \frac{1}{\sqrt{2}}(F_\pi - 2F_K). \quad (30)$$

With an increase of the baryon density the values of  $\sigma$  and  $\zeta$  rise which in turn result in a decrease of the effective baryon masses. The effective baryon mass  $M_j^*$  are generally in the region

$$0 \leq M_j^*(\sigma, \zeta) \leq M_j(\sigma_0, \zeta_0). \quad (31)$$

The ranges of mean field values for  $\sigma$  and  $\zeta$  are set by

$$\sigma_0 \leq \sigma \leq \sigma_b, \quad \zeta_0 \leq \zeta \leq \zeta_b, \quad (32)$$

where the upper values  $\sigma_b$  and  $\zeta_b$  are determined by  $M_N^* = 0$ ,  $M_\Lambda^* = 0$  or  $M_\Xi^* = 0$ . Since the  $\Sigma$  hyperon has the same quark flavor content as the  $\Lambda$ , its effective mass is always larger than that of the  $\Lambda$ . At a specific point for high baryon density, the minimum of the thermodynamical potential  $\Omega$  appears not inside the region, but at the boundary of values given for  $\sigma$  and  $\zeta$ . In this limit, the equations (27) and (28) for  $\sigma$  and  $\zeta$  are not valid any more. At the boundary, the mean fields  $\sigma$  and  $\zeta$  satisfy the equations

$$\frac{\partial \Omega}{\partial Z} = 0, \quad dZ = \sqrt{d\sigma^2 + d\zeta^2}, \quad (33)$$

where  $Z$  is in the boundary and  $d\sigma$ ,  $d\zeta$  are constraint by

$$\frac{\partial M_j^*(\sigma, \zeta)}{\partial \sigma} d\sigma + \frac{\partial M_j^*(\sigma, \zeta)}{\partial \zeta} d\zeta = 0 \quad (j = N, \Lambda, \Xi). \quad (34)$$

Therefore, if the minimum of the thermodynamical potential appears for  $M_j^*(\sigma, \zeta) = 0$ , the equations of  $\sigma$  and  $\zeta$  are

$$M_j^*(\sigma, \zeta) = 0, \quad (35)$$

$$\frac{\partial \Omega}{\partial \sigma} \frac{1}{\sqrt{1 + \left(\frac{\partial M_j^*/\partial \sigma}{\partial M_j^*/\partial \zeta}\right)^2}} + \frac{\partial \Omega}{\partial \zeta} \frac{1}{\sqrt{1 + \left(\frac{\partial M_j^*/\partial \zeta}{\partial M_j^*/\partial \sigma}\right)^2}} = 0. \quad (36)$$

For the special case, when  $M_N^*$  is only a function of  $\sigma$ , equation (36) will be the same as equation (28).

## IV. NUMERICAL RESULTS

The parameters of the chiral SU(3) quark mean field model are determined, as previously done [26,27], by the meson masses in vacuum and the properties of nuclear matter. The confining potential  $\chi_c$ , is chosen as in Refs. [27,29] which, in comparison with other two types of potentials is the best to describe finite systems. A list of the model parameters is contained in table I. In the previous section, we already mentioned that the values of  $\sigma$  and  $\zeta$  are determined by minimization of the thermodynamical potential  $\Omega$ . At zero temperature, the scalar meson mean field values can be obtained by minimizing the energy per volume  $\varepsilon$ . For nonstrange matter,  $\varepsilon$  can be expressed as a function of  $\sigma$  or of the effective nucleon mass  $M_N^*$ . At some critical baryon density the minimum of  $\varepsilon$  appears at  $M_N^* = 0$ , a scenario which has been studied in Ref. [29]. For strange hadronic matter  $\varepsilon$  is a function of the mean field values  $\sigma$  and  $\zeta$ . In Fig. 1, we indicate the results for the energy density  $\varepsilon$  versus  $\sigma$  and  $\zeta$  at a baryon density of  $\rho_B = 0.3 \text{ fm}^{-3}$  and for a strangeness fraction of  $f_s = 1.0$ . A minimum for  $\varepsilon$  is obtained for values of the scalar fields with  $\sigma \simeq -0.24 \text{ fm}^{-1}$  and  $\zeta \simeq -0.34 \text{ fm}^{-1}$ . The corresponding effective nucleon and hyperon masses have nonzero values. In most other models, for any values of the strangeness fraction and the baryon density, a solution for the mean field equations corresponding to (27) and (28), can be obtained, that is the minimum of  $\varepsilon$  occurs for nonzero effective baryon masses. However, in the present chiral SU(3) quark mean field model, the minimum of  $\varepsilon$  will appear on the boundary of  $\sigma$  and  $\zeta$  at high baryon density for a fixed strangeness fraction.

In Fig. 2 we plot the boundary of  $\sigma$  and  $\zeta$  resulting from the model. The solid, dashed and dotted lines correspond to the three boundaries where the effective baryon masses are zero, i.e.,  $M_N^* = 0$ ,  $M_\Lambda^* = 0$  and  $M_\Xi^* = 0$ . The two coordinate axis and the three boundaries form an area ABCDE. Inside this area, the effective baryon masses are nonzero. On the boundary the dynamical equations (27) and (28) for  $\sigma$  and  $\zeta$  have to be replaced by equations (35) and (36). The numerical calculations show that for small strangeness fraction and at sufficiently high baryon density the minimum of  $\varepsilon$  corresponds to the case of the solid line with a vanishing effective nucleon mass. For large strangeness fraction, the minimum of  $\varepsilon$  will coincide with the dotted line defined by a zero effective mass of the  $\Xi$  hyperon. The minimum of  $\varepsilon$  will never correspond to case of the dashed line (except at the points B and C) where only  $M_\Lambda^*$  vanishes. At the point B both  $M_N^*$  and  $M_\Lambda^*$  are zero, whereas point C is set by vanishing values of  $M_\Lambda^*$  and  $M_\Xi^*$ .

We next discuss the change of the effective baryon masses in dependence on the baryon density. In Fig. 3, we plot the effective baryon masses versus density at a strangeness fraction of  $f_s = 0.8$ . As in most other models, the effective baryon masses decrease with increasing baryon density. At this value for the strangeness fraction, the effective mass of the nucleon decreases faster than those of the other baryons. On the contrary, the effective  $\Xi$  mass decreases slower. This is because when the strangeness is small, the interaction between non-strange quarks and the  $\sigma$  meson is considerably stronger than the one between strange quarks and  $\zeta$ . When the baryon density  $\rho_B$  reaches a value of  $0.46 \text{ fm}^{-3}$ , the effective nucleon mass drops from 0.2 GeV to zero. All other effective baryon masses also decrease discontinuously, but in these cases to finite values. In the range of  $0.46 \text{ fm}^{-3} < \rho_B < 0.69 \text{ fm}^{-3}$  the effective hyperon masses continue to decrease. When the density is larger than  $0.69 \text{ fm}^{-3}$ , both nucleon and  $\Lambda$  masses equal zero while the  $\Sigma$  and  $\Xi$  masses remain at a

constant and finite value.

The density dependence of the baryon masses sensitively depends on the strangeness fraction. For high strangeness fraction, the interaction between hyperons is stronger than the one between nucleons. The effective masses of hyperons with a larger strange quark content will therefore decrease faster. As a result, at a high value of the baryon density, the hyperon masses will be zero, while the nucleon mass is still finite. This effect is clearly seen from Fig. 4, where we plot the phase diagram. For the case of nonstrange hadronic matter, there are only two phases. One normal phase, where chiral symmetry is spontaneously broken, whereas at high density we have chiral symmetry restoration phase with a zero effective nucleon mass. Strange hadronic matter, corresponds to the additional presence of  $\Lambda$ ,  $\Sigma$  and  $\Xi$  hyperons. Because the effective masses of the baryons drop to zero at different values of the baryon density and strangeness fraction, we obtain different chiral symmetry restoration phases. The rich phase structure is illustrated in Fig. 4 with five qualitatively different regions. Phase I refers to the normal phase with nonzero baryon masses. In the chiral symmetry restoration phase II, only the effective nucleon mass is zero. In phase III, both nucleon and  $\Lambda$  masses are vanishing. Phase IV, designates the case where both  $\Lambda$  and  $\Xi$  have zero effective masses, whereas phase V only has a vanishing value for  $M_{\Xi}^*$ . For different value of the strangeness fraction  $f_s$ , the normal phase I will turn into different chiral symmetry restoration phases at different critical densities. For nonstrange nuclear matter the critical baryon density is reached at a value of  $0.28 \text{ fm}^{-3}$ , where the system will be in phase II. For values of the strangeness fraction with  $f_s < 1.0$ , the critical density increases with growing  $f_s$ . The maximum of the critical density of about  $0.5 \text{ fm}^{-3}$  is reached for  $f_s \simeq 1.0$ . For the range of values  $0.6 < f_s < 1.1$ , when the baryon density is high enough, the chiral restoration phase can furthermore change from phase II to phase III. For larger values of the strangeness fraction, that is  $f_s > 1.1$ , the effective nucleon mass will not drop to zero at any density. In the range of  $1.1 < f_s < 1.3$ , when the density reaches a critical point, the system changes directly from phase I to phase III. At some higher density, a further transition from phase III into phase IV takes places. For  $1.3 < f_s < 1.75$ , the normal phase I changes into phase IV at the critical point. For  $f_s > 1.75$ , chiral symmetry restoration is manifest only in phase V.

In Fig. 5, we plot the energy per baryon  $E/A$  in dependence on the baryon density for different strangeness fractions. For normal nuclear matter the binding energy is 16 MeV at the saturation density  $\rho_0$  of  $0.16 \text{ fm}^{-3}$ . When the density reaches a value of about  $0.28 \text{ fm}^{-3}$ , a discontinuous decrease of energy per baryon occurs. At  $\rho_B \simeq 0.31 \text{ fm}^{-3}$  there is a second minimum for  $E/A$  which is close to -16 MeV. When the density is larger than about  $0.31 \text{ fm}^{-3}$  the energy per baryon increases with growing density. As the strangeness fraction increases, the first minimum of  $E/A$  first increases and then decreases. At  $f_s \simeq 1.2$ , the first maximum of the binding energy is about 19 MeV. The binding energy at the second minimum is about 70 MeV and the corresponding  $f_s$  is about 1.5. The system therefore favors to have a large strangeness fraction where the corresponding density is about 3-4 times that of the saturation density  $\rho_0$  of normal nuclear matter.

## V. SUMMARY

We applied the chiral SU(3) quark mean field model to investigate the mechanism of chiral symmetry restoration in strange hadronic matter. The model is based on effective quark-meson and meson self-interactions which satisfy the chiral SU(3) symmetry constraint. Chiral symmetry restoration of nonstrange nuclear matter was studied in a previous paper [29]. When a critical baryon density is reached, the effective nucleon mass will drop to zero. This phenomenon is related to the fact that nuclear matter has its lowest energy per volume in the chiral symmetry restoration phase at high density.

In the present work we extended the discussion to strange hadronic systems including  $\Lambda$ ,  $\Sigma$  and  $\Xi$  hyperons. As for the case of nonstrange nuclear matter, when the baryon density is sufficient high, the minimum of the energy per volume  $\varepsilon$  of strange matter will occur for effective baryon masses reaching a vanishing value. As it turns out, the effective masses of the different baryons do not change to zero at the same value of baryon density and strangeness fraction. In the effective model there occur four different chiral symmetry restoration phases which are characterized by zero effective masses of the different baryons. For a given strangeness fraction, when the baryon density is larger than the critical density, hadronic matter will make a transition to the corresponding chiral symmetry restoration phase with values for the critical density which is about 2-3 times larger than the nuclear saturation density  $\rho_0$ .

The energy per baryon  $E/A$  has two minima for a given strangeness fraction. One corresponds to the normal phase, the other one occurs for the chiral symmetry restoration phase. For small strangeness fraction, that is  $f_s < 1.0$ , the minimum of  $E/A$  in the normal phase is lower than the one of the restored phase. For large strangeness fraction the system is favored to be in the chiral symmetry restoration phase since it occurs with a larger binding energy. The maximal binding energy is about 70 MeV for a strangeness fraction of about 1.5.

The deconfinement phase transition may also occur at high densities. It is worthwhile to study whether the phase transition between hadronic and quark matter also takes place at values for the baryon densities which are close to the ones when chiral symmetry restoration occurs. Both the quark and the hadronic phase can be described in the chiral SU(3) quark mean field model. The model therefore opens up the possibility to also study the deconfinement phase transition, a topic which will be pursued in future studies.

### Acknowledgments

P. W. would like to thank the Institute for Theoretical Physics, University of Tübingen for their hospitality. This work was supported by the Alexander von Humboldt Foundation and by the DFG under contracts FA67/25-3, GRK683.

## REFERENCES

- [1] B. Müller, Nucl. Phys. A **661** (1999) 272.
- [2] U. Heinz, hep-ph/9902424.
- [3] F. Karsch, hep-lat/9903031.
- [4] C. Wetterich, Phys. Rev. D **66** (2002) 056003.
- [5] P. Koch, B. Müller, and J. Rafelski, Phys. Rep. **142** (1986) 167.
- [6] M. Gonin *et al.* [NA50 Collaboration], Nucl. Phys. A **610** (1996) 404c.
- [7] D. Ardouin *et al.*, Phys. Lett. B **446** (1999) 191.
- [8] M. Asakawa, U. W. Heinz, and B. Muller, Phys. Rev. Lett. **85** (2000) 2072.
- [9] T. A. Armstrong *et al.*, Phys. Rev. C **59** (1999) 1829.
- [10] M. C. Abreu *et al.* [NA50 Collaboration], Phys. Lett. B **477** (2000) 28.
- [11] P. J. de A. Bicudo, Phys. Rev. Lett **72** (1994) 1600.
- [12] T. D. Cohen, R. J. Furnstahl, and K. Griegel, Phys. Rev. C **45** (1992) 1881.
- [13] G. Q. Li and C. M. Ko, Phys. Lett. B **338** (1994) 118.
- [14] R. Brockmann and W. Weise, Phys. Lett. B **367** (1996) 40.
- [15] T. Mitsumori, N. Noda, H. Kouno, A. Hasegawa, and M. Nakano, Phys. Rev. C **55** (1997) 1577.
- [16] G. E. Brown and M. Rho, Phys. Rev. Lett. **66** (1991) 272.
- [17] E. K. Heide, S. Rudaz, and P. J. Ellis, Nucl. Phys. A **571** (1994) 713.
- [18] G. Carter, P. J. Ellis, and S. Rudaz, Nucl. Phys. A **603** (1996) 367; Erratum-ibid. **A608** (1996) 514.
- [19] R. J. Furnstahl, H. B. Tang, and B. D. Serot, Phys. Rev. C **52** (1995) 1368.
- [20] I. Mishustin, J. Bondorf, and M. Rho, Nucl. Phys. A **555** (1993) 215.
- [21] P. Papazoglou, J. Schaffner, S. Schramm, D. Zschesche, H. Stöcker, and W. Greiner, Phys. Rev. C **55** (1997) 1499.
- [22] L. L. Zhang, H. Q. Song, P. Wang, and R. K. Su, Phys. Rev. C **59** (1999) 3292.
- [23] P. Wang, Phys. Rev. C **61** (2000) 054904.
- [24] P. Papazoglou, S. Schramm, J. Schaffner-Bielich, H. Stöcker, and W. Greiner, Phys. Rev. C **57** (1998) 2576.
- [25] P. Papazoglou, D. Zschesche, S. Schramm, J. Schaffner-Bielich, H. Stöcker, and W. Greiner, Phys. Rev. C **59** (1999) 411.
- [26] P. Wang, Z. Y. Zhang, Y. W. Yu, R. K. Su, and H. Q. Song, Nucl. Phys. A **688** (2001) 791.
- [27] P. Wang, H. Guo, Z. Y. Zhang, Y. W. Yu, R. K. Su, and H. Q. Song, Nucl. Phys. A **705** (2002) 455.
- [28] P. Wang, V. E. Lyubovitskij, Th. Gutsche, and A. Faessler, Phys. Rev. C **67** (2003) 015210.
- [29] P. Wang, H. Guo, Y. B. Dong, Z. Y. Zhang, and Y. W. Yu, J. Phys. G **28** (2002) 2265.

### Figure captions

Fig.1. The energy per volume  $\varepsilon$  of strange hadronic matter versus  $\sigma$  and  $\zeta$  with  $\rho_B = 0.3$   $\text{fm}^{-3}$  and  $f_s = 1.0$ .

Fig.2. The boundary of  $\sigma$  and  $\zeta$ . The solid, dashed and dotted lines are the boundaries for  $M_N^* = 0$ ,  $M_\Lambda^* = 0$  and  $M_\Xi^* = 0$ , respectively.

Fig.3. The effective baryon masses versus baryon density with  $f_s = 0.8$ . The solid, dashed, dotted and dash-dotted lines are for nucleon,  $\Lambda$ ,  $\Sigma$  and  $\Xi$ , respectively.

Fig.4. The phase diagram for strange hadronic matter. Phase I is the normal phase. Phase II, III, IV and V are the chiral symmetry restoration phases with  $M_N^* = 0$ ,  $M_N^* = M_\Lambda^* = 0$ ,  $M_\Lambda^* = M_\Xi^* = 0$  and  $M_\Xi^* = 0$ , respectively.

Fig.5. The energy per baryon  $E/A$  versus baryon density  $\rho_B$  at different strangeness fractions.

## TABLES

TABLE I. Parameters of the model.

$k_0$	$k_1$	$k_2$	$k_3$	$k_4$	$g_s$	$g_v$	$g_4$	$h_1$	$h_2$
4.21	2.26	-10.16	-4.38	-0.13	4.76	10.37	7.5	-2.07	3.16

FIGURES

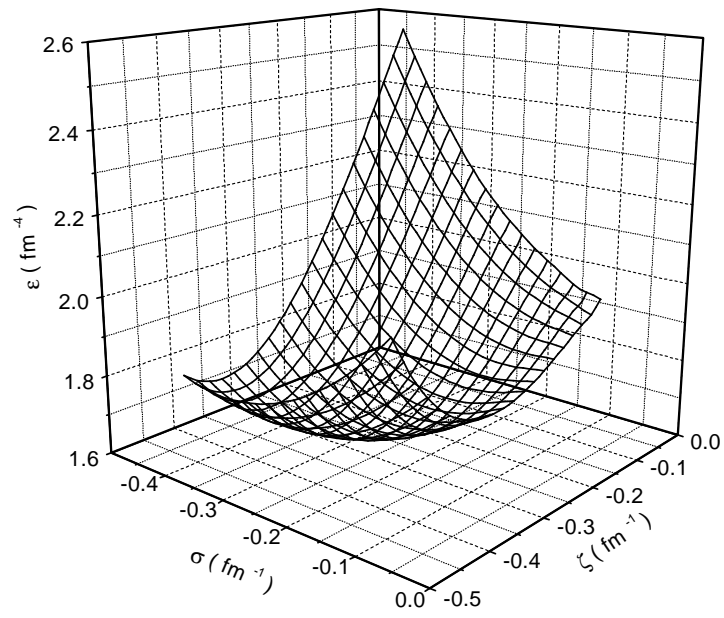


Fig. 1

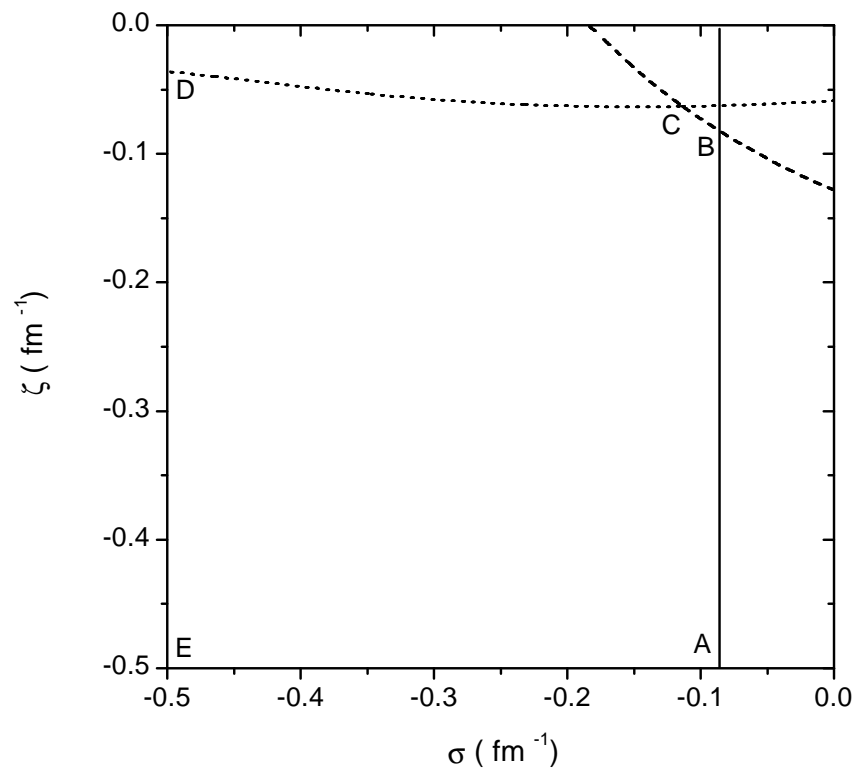


Fig. 2

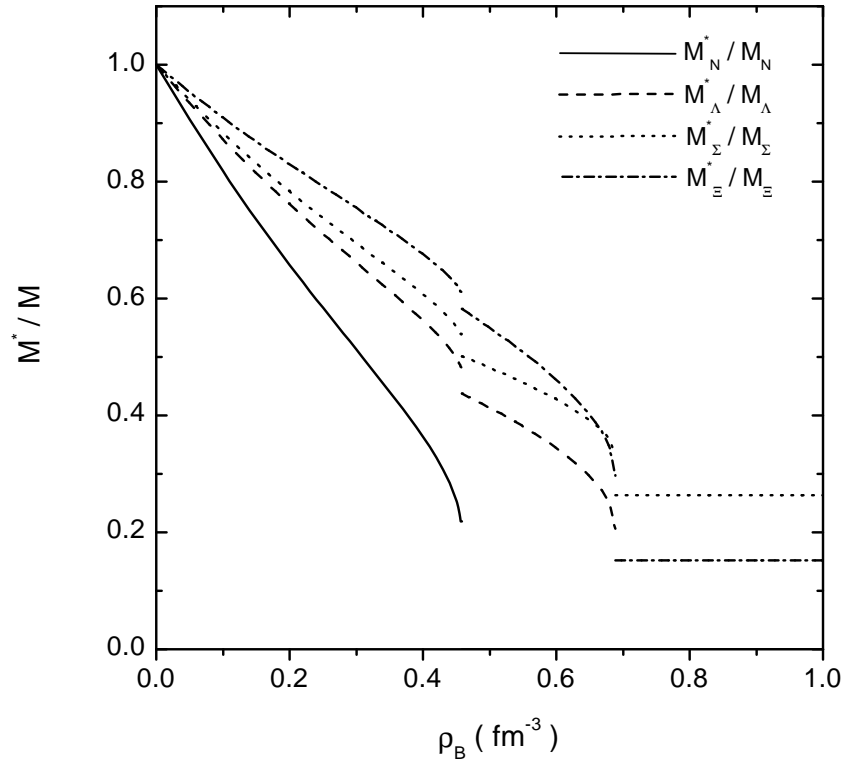


Fig. 3

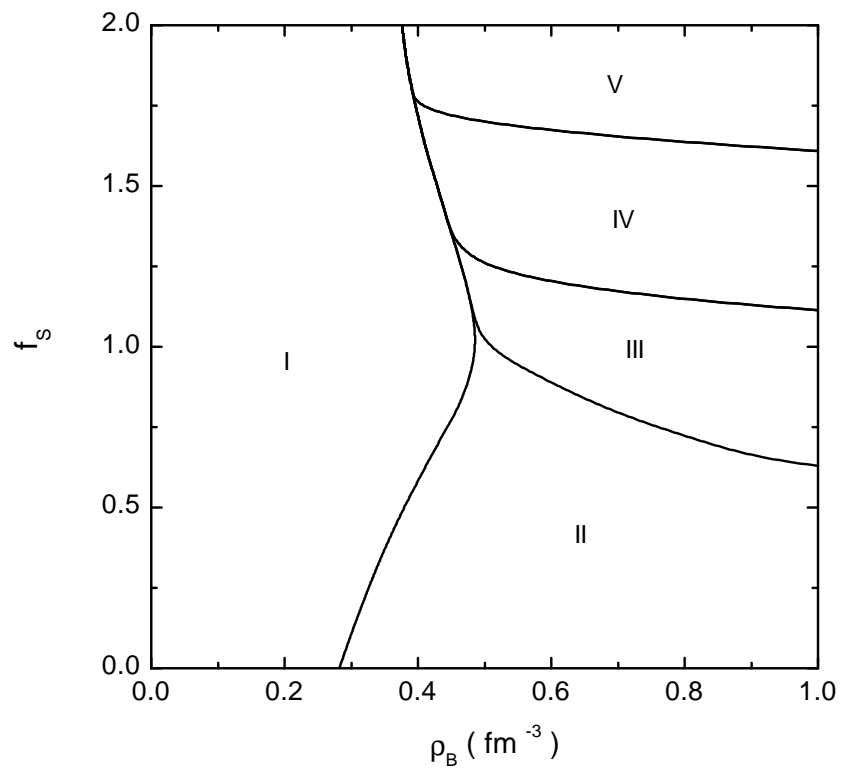


Fig. 4

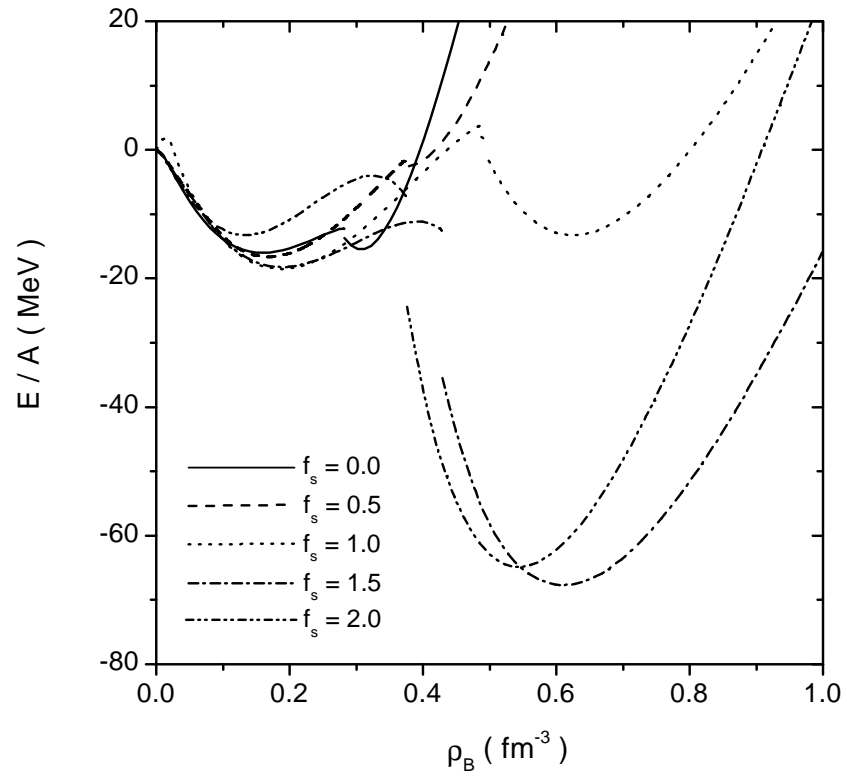


Fig. 5